

Figure 53. Entrance on Khnum-Khufu. (a): Optical image. (b): Tomographic map (magnitude).

5.17. Big Void (Tag 19)

This is a large structure whose shape resembles a parallelepiped (number 19 of the 3D model). This object appears to be connected to structure 10 by means of a double horizontal connection (number 20 of the 3D model). The reference tomography images are shown in Figures 55b and 56b, while the 3D models are depicted in Figure 55a and 56a. The large red target 1 visible in Figure 56b is a false alarm, which is generated by the southwest ascending angle of the pyramid [69].

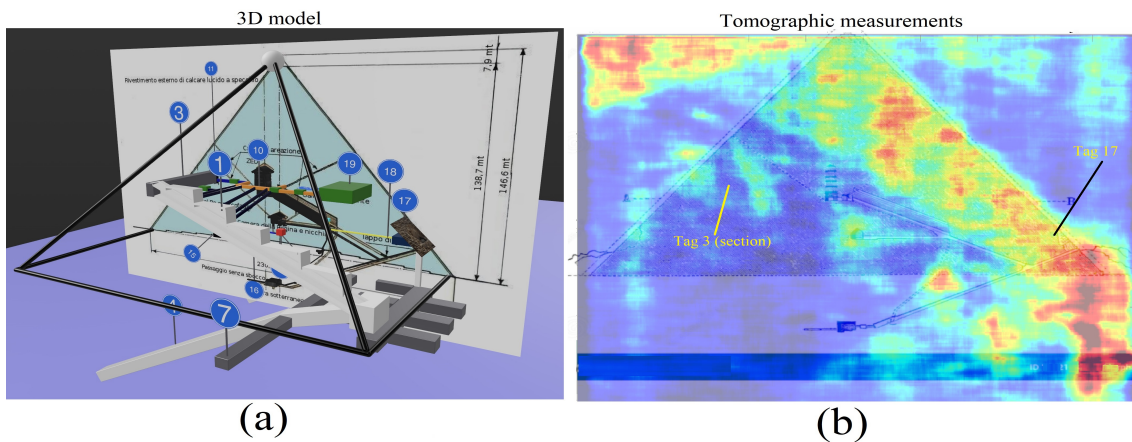


Figure 54. Tags association from tomography to 3D model. (a): Three-dimensional (3D) model of Khnum-Khufu. (b): Tomographic reconstruction (magnitude).

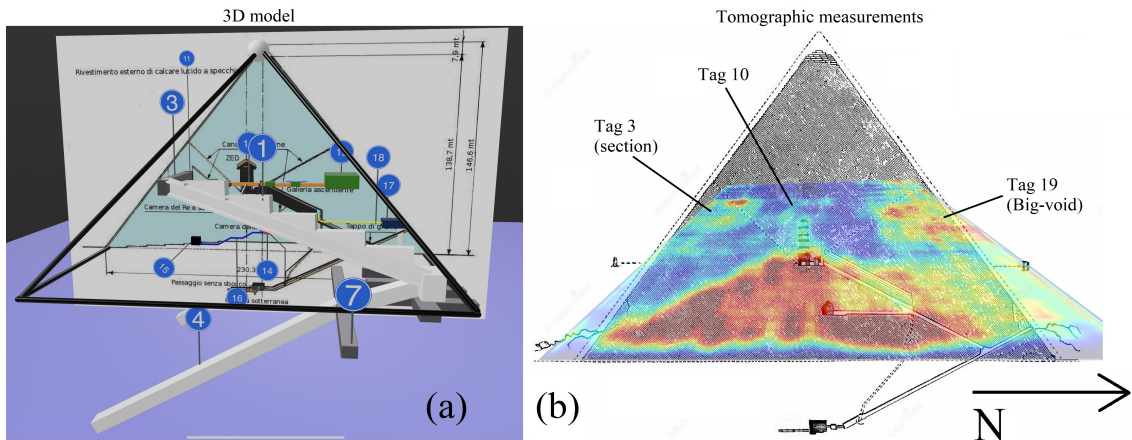


Figure 55. Tags association from tomography to 3D model. (a): Three-dimensional (3D) model of Khnum-Khufu. (b): Tomographic reconstruction (magnitude).

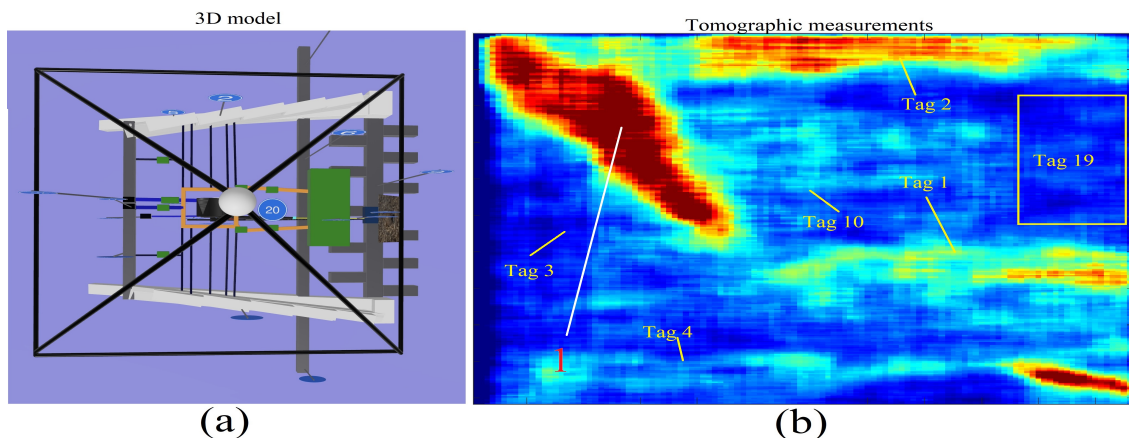


Figure 56. Tags association from tomography to 3D model. **(a)**: Three-dimensional (3D) model of Khnum-Khufu. **(b)**: Tomographic reconstruction (magnitude).

5.18. Zed-Big Void Double Connection (Tag 20)

Structure 19 (big void) is connected to the large corridor 3 to the south, at the height of the big void, via two oblique corridors. The reference tomography is shown in Figure 41b, while the reference 3D model is shown in Figure 49a.

5.19. Metric Determination

The final objective of this study is to provide approximate measurements of the structures detected using the Doppler SAR tomography technique. The measurements that we propose are expressed in meters and are affected by an error that we have estimated to be very low, with respect to the actual measurement of the structures, according to the particular methodology we used. The dimensions are proposed in Figures 57–59. The measurements we suggest also include the thickness of the material used to construct them and are not to be intended as mere empty space. With regard to obtaining only empty space, research is currently underway in order to improve the technique and find a way to distinguish solid spaces from hollow spaces. The measures reported are evaluated by using Tape Measuring Wall Area software (<http://www.pictureenginecompany.com/MeasureEngine/Promo.html> (accessed on 1 July 2022)) employing as internal standard the pyramid's base length and are in accordance with the results afforded by SAR data.

Table 5. List of the principal tomographic images.

| Picture | Tomographic Looking-Direction | Tomographic Line Orientation |
|-----------|-------------------------------|------------------------------|
| Figure 29 | Eastern-side | Vertical |
| Figure 30 | Northern side | Horizontal |
| Figure 31 | Western side | Horizontal |
| Figure 32 | Eastern side | Horizontal |
| Figure 33 | Western side | Horizontal |
| Figure 34 | Northern side | Horizontal |
| Figure 35 | Western side | Vertical |
| Figure 36 | Eastern side | Vertical investigation |
| Figure 37 | Northern–Southern side | Vertical |
| Figure 38 | Southern side | Horizontal |

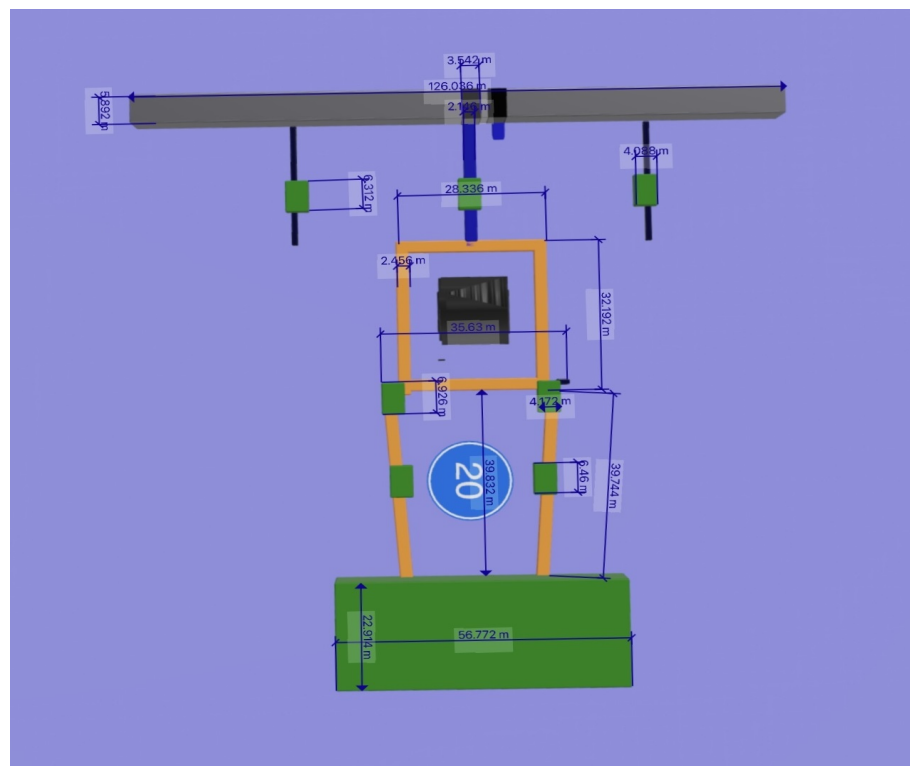


Figure 57. Measurements of the detected facilities of the pyramid. The numbers shown after the comma cannot be significant. (Top-side view).

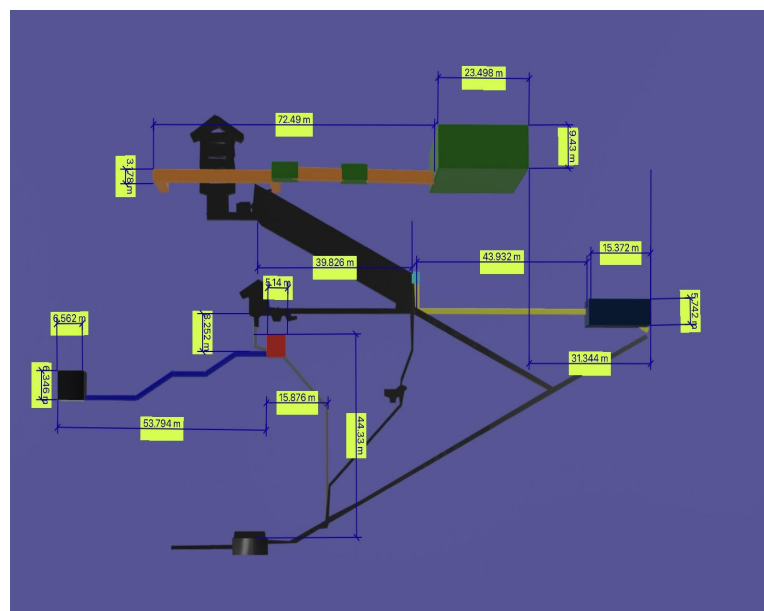


Figure 58. Measurements of the detected facilities of the pyramid. The numbers shown after the comma cannot be significant. (East-side view).

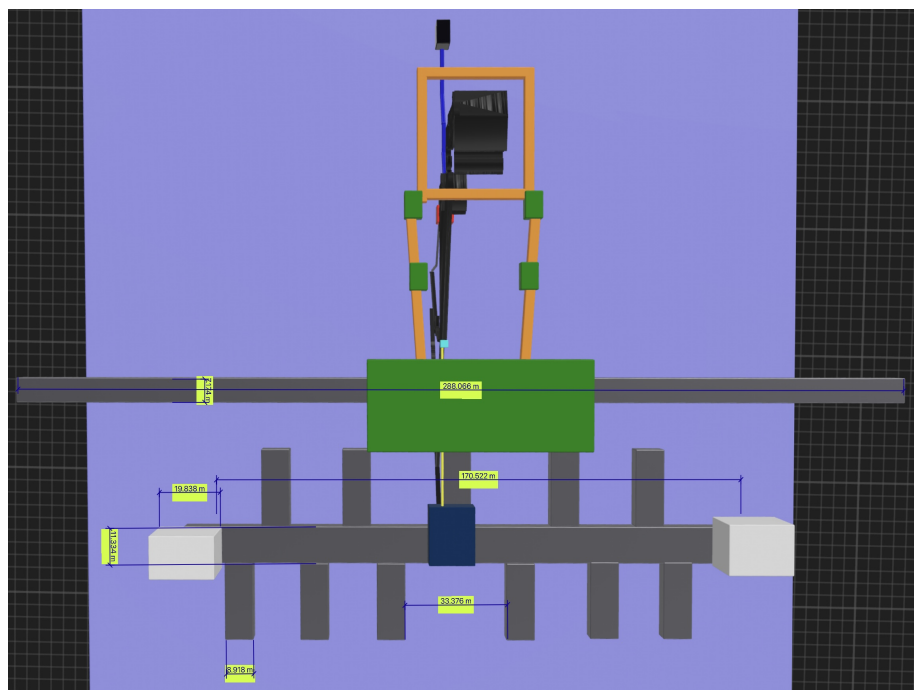


Figure 59. Measurements of the detected facilities of the pyramid. The numbers shown after the comma cannot be significant. (Top-side particular view).

6. Discussion

6.1. Data Analysis

Here, we proceed to data analysis, while being aware that some aspects of the internal structure of the pyramid of Khnum-Khufu still need to be clarified; it is possible, in our opinion, to attribute a meaning to the internal structures of the monument, taking into account all the data relating to previous research in this field. It is possible to underline how our 3D reconstruction, even if for now it does not claim to indicate the true measurements of the objects shown (even if the SAR technique can accurately evaluate this parameter), is following some facts exposed in previous research. Some researchers have shown how on the north edge of the east side of the pyramid at ground level, there is a thermal anomaly that suggests the presence of a room and a corridor located a few meters from the external wall of the monument [36,38,39,70]. These data are in agreement with our analyses which predict, at that point, the presence of a room as a link between the two ramps 1 and 4 of our 3D model. The microgravimetry data, carried out on the pyramid by different research groups [33,34,36,37], can show us how, under the floor of the King's room, there is a lack of homogeneity possibly attributable to structures such as those hypothesized by us (see points 12 and 13 of the 3D model). The presence of rooms located under the King's room is also amply documented by many photographic findings on the Web. The presence of ramps, placed inside the pyramid and which we highlight with certainty for the first time (numbers 1, 2, 3, and 4 of the 3D model), had already been postulated [15] and partly detected by electrogravitic measurements carried out in 1998 [35]. The presence of further rooms located near the Queen's room had already been postulated in the past by some researchers [35,71]; however, this is based on intuitions not confirmed by objective evidence. The authors of [71] also postulated the presence of a horizontal passage placed between the original entrance of the pyramid and the Great Gallery, in place of structure number 17, which we highlight in this work; moreover, in this work, the presence of a room located immediately after the entrance to the great pyramid is highlighted. This void also seemed to be confirmed by muon spectroscopy [9] carried out by researchers at the University of Nagoya in 2017 and indicated with the name “small void”. It must be strongly emphasized that while the analyses used up to now in the attempt to describe the objects inside the pyramid gave only the possibility of making indirect hypotheses, the SAR methodology

visibly produces direct evidence of the geometries inside the objects that can be analyzed. In contrast, the muon spectroscopy used in 2017 [9] would not have been deemed reliable by the Egyptian Supreme Council of Antiquities, providing controversial data [41]. No trace of the presence of a structure identified as a big void, put in evidence by muonic spectroscopy [9], was in our hands detected by SAR. On the other hand, the SAR technique allows us to make more observations using different starting geometries, thus being able to see the same structures inside the pyramid, from different points of view, and the only possibility for a mistake lies in the visual interpretation of the data obtained but does not invalidate the presence or absence of specific structural elements. The geometries of the objects highlighted by the SAR in this paper also make us reasonably exclude any errors due to the possible non-homogeneity of the materials employed during the construction of the pyramid interiors.

6.2. Data Interpretation

On the basis of the above, it appears necessary to provide a plausible explanation as a key to understanding the function of the structures found inside the pyramid, taking into account that this interpretation is only intended to be a starting point for further interpretative ideas that could arise from a serene discussion at the level of the scientific community. The authors' vision starts from what we have already previously published in [72] and widely discussed [12,16,22,23,28,31,73–75]. Starting from the observation of the outside of the three pyramids of the Giza plateau, for the first time, we were able to establish that the three pyramids of Khnum-Khufu, Kefren and Menkaure have eight sides. This feature, known only for the larger pyramid, is now extended to the other two. According to the authors of [73], the idea that the pyramids of the Giza plateau had this characteristic is due to the need to convey, in an orderly manner, the water that flowed along the faces of the pyramidal structures. In the case of the pyramid of Khnum-Khufu, which we have analyzed in depth, it can be assumed, in analogy with other authors [5,25,76], that it was surrounded by an enormous basin full of water, which allowed the circulation of some boats. These boats were used by some attendants with the task of bringing the water to about 90 m high, pouring it into the south shaft by using many rotating stones probably similar to the Sabu diorite stone [28]. The SAR technique allows us to provide evidence that the shape of this monument does not resemble a perfect pyramidal form because of the presence of a double changing in slope: the first of which is 14.5 ca. degrees at approximately 20 m high, while the second one is 6 degrees ca. at approximately 100 m high. The Nile River's water should have filled the basin up to the height of the first change of slope of the pyramid, thus allowing the Egyptian boats not to get stuck with the keel on the side of the pyramid itself. The water would have invaded the King's chamber, but having reached the height of the granite basin inside the chamber (often referred to as the sarcophagus), it would not have exceeded that level in height and would have instead risen in the north shaft, whose entrance is placed at the same height as the basin, creating an air seal that effectively airlocked the room. Having the King's chamber in fact hermetically sealed would have caused excess water to rise up the north shaft. The Queen's chamber would also be filled with water, up to the height of the shafts, by means of two connections to the shafts of the King's chamber, which were probably located in rooms 19 and 11, building a closed circuit, which is called Quincke's tube [26]. As also proposed by other authors [77], the pyramid, with its megalithic structure, was placed in vibration by the wind and the low frequencies thus developed, which acted as a low-pass filter allowing only low frequencies to bounce back on the roof of the Zed toward the King's chamber [16]. Such a room would behave like an air-filled bottle of Helmholtz [29], in which the granite basin acted as a bottleneck. The walls of the basin, vibrating at low and precise frequencies, linked to the internal and external measurements of the basin itself, proportional to multiples of π and the Golden Ratio ϕ [16], would have caused the water contained in the Quincke's circuit to vibrate. These frequencies, traveling through the closed circuit of Quincke's tube, at about 1400 m/s (speed of sound in the water), reached the Queen's chamber, where the height of the water

could not exceed the height of shafts from the floor. A particular frequency could be developed, which was suitably amplified by the correct dimensions of the niche present in the west wall, which acted as a sound box for a musical instrument, releasing into the air a sound frequency that was able to interact with a cylindrical container placed on the floor of the room, the traces of which are still visible [14]. This cylindrical container, probably made of wood, was put into resonance by the obtained low frequency. Two individuals were placed both in the basin of the King's chamber and in the cylindrical container, in the Queen's chamber and appropriately treated with this low sound frequency for curative and religious purposes [21]. At the end of the procedure, the King's chamber was emptied by letting the water out of the Great Gallery and conveying it toward the room called "Grotto" toward the "Unfinished" chamber which brought the water back through a path in the floor, now occluded by debris, to the Nile. Subsequently, the Queen's chamber was emptied in two steps: first, a granite "plug" in the corridor leading to the room was removed: (this passage actually has a slight hydraulic slope toward the Great Gallery) and the water was made to flow out, at the floor of the Great Gallery, where it was conveyed toward the "Grotto". Subsequently, a plug placed in the floor was removed to finish the emptying of the room. The water thus conveyed through the hole in the floor, highlighted in a book published in 1877 [14], allowed the liquid to enter the room which, in our 3D reconstruction, corresponds to the number 14, eventually reaching the "Unfinished" room and returning to the Nile. The "Grotto" and room 14 are, in our opinion, necessary to stop the fall of water by slowing down its speed, with a mechanism similar to a common water jet pump used in laboratories to create vacuum in equipment, which is called Venturi's tube. The evident traces of erosion due to water inside the pyramid rooms are in support of our interpretative hypothesis. The three boulders that today are wedged at the beginning of the oblique corridor leading to the Great Gallery would have been used as "plugs" to block the access of water to the exit of the pyramid or from the Queen's chamber by making them flow in different positions as needed. The existence of passage 18 seems to be related to a little open room, which has never been described by anyone but is well tracked by photographic evidence, that appears located at the top of the entrance of the Great Gallery and was probably employed as security exit. The entire system of the ramps highlighted by the SAR could be interpreted as a gigantic resonant structure, having the purpose of equalizing any differences in vibration between the north and south part of the pyramid, with the aim of making the square structure reach number 10, placed around the Zed, an equalized vibrational signal. Similarly, the complex structure number 9 identified immediately below the plane on which the pyramid rests has a shape similar to structures used to absorb the effects of mechanical vibrations that are transmitted through the ground [30]. The technique proposed in this article, unlike the classical SAR tomography developed in [52,64,65], has penetration properties orders of magnitude greater because what is proposed uses the vibrations (the phonons) and not the photonic information. A disadvantage of the present technique could be the processing time needed to carry out vibrational raw data synthesis, which requires substantial computing resources. As an example, to collect a full resolution tomogram, e.g., the one in Figure 46b, using a DELL i7 PC with 32 GB of RAM installed, took approximately 6 days of computational time.

7. Conclusions

In this paper, we have shown how it is possible to use SAR MM Doppler tomography in an advantageous, economical, non-invasive and rapid way to make a valid contribution in the study of the structure of ancient megalithic monuments such as the pyramid of Khnum-Khufu. We are aware that only by confirmation on the field of our findings can we validate our hypothesis. However, it seemed logical to provide a hypothetical interpretation based on the data we collected that could serve as a starting point for future research.

From our point of view, the results obtained on the pyramid of Khnum-Khufu must be considered in their entirety (globally and not locally), thus taking into account the new structures found within it, the existence of which was previously unknown, all of which are

connected. We have also discovered and measured that the pyramids of the Giza Plateau present, on all faces, spatial indentations that tend to divide them in two with respect to the axes of central symmetry, constituted by their vertices. In this context, it seems clear that the multitude of structures, together with the octagonal feature of Khnum-Khufu, are to be seen as connected features. The numerous structures thus seem to belong to a gigantic resonator with the Zed that, in our personal opinion, could function as a high-order (probably fifth-order) low-pass acoustic filter due to its multi-layer and hence multi-stage characteristic. At the time of the construction of the pyramids, the Nile most probably reached the Giza plain, and the pyramids were probably flooded with water up to a couple of meters from their base. This explains why rowing boats were found without masts to support the sails. Once we have consolidated this article, we will need to provide an add-on explaining in detail the function of each chamber. At this point, it might not be at all wrong to assume that many of the structures inside the pyramid could have been purposely flooded several times a year and thus left with the liquid flowing inside. The excess water could then be expelled from the shafts, which then, thanks to the distortions on the faces (those estimated from the external results), acted as conveyors, so that the water could be transported by gravity to the ground in an orderly manner. By looking at the estimated tomographs, we were able to realize that the inner areas could be reached safely from a precise point identified by the entrance corridor on the north side (Tag 17). From our point of view, it is possible to open a minimally invasive passageway, which is the way to the exploration of all structures surveyed. This could be completed simply by drilling a passage from the main entrance (i.e., by drilling Tag 18).

In addition, the work carried out on Khnum-Khufu will certainly be extended to look inside other megalithic structures, even those belonging to other continents. At present, the research team is carrying out the same work as for Khnum-Khufu, but extended to the pyramid of Khefren, in order to have a more complete overview of the megalithic apparatus of Giza. We are confident that we will also provide Khefren's internal results in the near future. In conclusion, through these discoveries, we believe it is appropriate for the Egyptian Authorities to begin a campaign of excavations and drilling in order to bring to light and give back to all humanity all the structures we estimated through the use of the proposed method.

In the near future, we would like to extend the SAR methodology to the investigation of the internal structure of other important monuments of the Giza plateau.

Author Contributions: The authors contributed to all parts of this work. All authors have read and agreed to the published version of the manuscript.

Funding: This research received no external funding.

Data Availability Statement: Not applicable.

Acknowledgments: We would like to thank Daniele Perissin for making the SARPROZ software available, through which many calculations were carried out more easily and quickly. We also thank the Italian Space Agency for providing the SAR data. We would also like to thank Riccardo Garzelli for conducting a deep revision of the English language and for having made crucial revisions to the entire article's structure and layout. The signal processing technique presented in this work has been submitted in patent application in 4 July 2022, to Commerce Department of Malta, Industrial Property Registrations Directorate, patent application number 4451. Additional information on the technique used and consultation of other experiments can be found at www.harmonicsar.com (accessed on 1 July 2022).

Conflicts of Interest: The authors declare no conflict of interest.

References

- Lehner, M.; Wilkinson, R.H. *Complete Pyramids: Solving the Ancient Mysteries*; Thames and Hudson Incorporated: London, UK, 1997.
- Hawass, Z. Pyramid construction: New evidence discovered in Giza. In *Stationen: Beiträge zur Kulturgeschichte*; Rainer Stadelmann gewidmet/hrsg. von Heike Guksch und Daniel Polz.-Mainz: von Zabern, Germany, 1998; ISBN 3-8053-2526-6.

3. Smith, C.B.; Hawass, Z. *How the Great Pyramid Was Built*; Smithsonian Institution: Washington, DC, USA, 2018.
4. Tallet, P.; Marouard, G. The harbor facilities of king Khufu on the Red Sea shore: The Wadi al-Jarf/Tell Ras Budran system. *J. Am. Res. Cent. Egypt* **2016**, *52*, 135–177. [[CrossRef](#)]
5. Bhatt, U. Subcontinent of india: A part of the earliest and most advanced civilisation of the world. *Int. J. Soc. Sci.* **2019**, *5*, 918–927. [[CrossRef](#)]
6. Kump, L.R. Foreshadowing the glacial era. *Nature* **2005**, *436*, 333–334. [[CrossRef](#)]
7. Bergendorff, S. *The Social and Cultural Order of Ancient Egypt: An Ethnographic and Regional Analysis*; Lexington Books: Washington, DC, USA, 2019.
8. Noc, E. Analyse Spatiale à Saqqâra des Origines à la fin de l’Ancien Empire: Les Exemples des Complexes Funéraires de Netjerikhet et de Sekhemkhet. Ph.D. Thesis, Montpellier 3, Montpellier, France, 2015.
9. Houdin, J.P. *La Construction de la Grande Pyramide*; PICARD DIFFUSES: Montluçon, France, 2007; Volume 150, ISBN 978-2910342456.
10. Baud, M. *Djéser et la IIIe Dynastie*; Pygmalion—Editions Pygmalion: Paris, France, 2015; ISBN 2-85704-779-7.
11. Dodson, A. The Layer Pyramid of Zawiyet el-Aryan: Its layout and context. *J. Am. Res. Cent. Egypt* **2000**, *37*, 81–90. [[CrossRef](#)]
12. Barsoum, M.; Ganguly, A.; Hug, G. Microstructural evidence of reconstituted limestone blocks in the Great Pyramids of Egypt. *J. Am. Ceram. Soc.* **2006**, *89*, 3788–3796. [[CrossRef](#)]
13. Harrell, J.A.; Penrod, B.E. The great pyramid debate—Evidence from the Lauer sample. *J. Geol. Educ.* **1993**, *41*, 358–363. [[CrossRef](#)]
14. Smyth, C.P. *Our Inheritance in the Great Pyramid*; W. Isbister: London, UK, 1877.
15. Tasellari, A.; Kaiku, E. How the Great Pyramid of Giza was built. An Engineering View. In Proceedings of the International Student Conference of Civil Engineering, Tirana, Albania, 11 May 2012.
16. Malanga, C. *Cheope la Fabbrica Dell’immortalità*; Spaziointeriore: Rome, Italy, 2020.
17. Hancock, G. *Fingerprints of the Gods*; Random House: New York, NY, USA, 2011.
18. Bedard, A.; Georges, T. Atmospheric infrasound. *Acoust. Aust.* **2000**, *28*, 47–52. [[CrossRef](#)]
19. Gossard, E.E.; Hooke, W.H. *Waves in the Atmosphere: Atmospheric Infrasound and Gravity Waves-Their Generation and Propagation*; Developments in Atmospheric Science No. 2; Elsevier: Amsterdam, The Netherlands, 1975.
20. De Carlo, M.; Arduin, F.; Le Pichon, A. Atmospheric infrasound generation by ocean waves in finite depth: Unified theory and application to radiation patterns. *Geophys. J. Int.* **2020**, *221*, 569–585. [[CrossRef](#)]
21. Till, R. Sound Archaeology: A Study of the Acoustics of Three World Heritage Sites, Spanish Prehistoric Painted Caves, Stonehenge, and Paphos Theatre. *Acoustics* **2019**, *1*, 661–692. [[CrossRef](#)]
22. Henry, S.; Di Borgo, E.P.; Danquigny, C.; Cavaillou, A.; Cottle, A.; Gaffet, S.; Pipe, M. Monitoring geomagnetic signals of groundwater movement using multiple underground SQUID magnetometers. *E3S Web Conf.* **2014**, *4*, 02004. [[CrossRef](#)]
23. Jouniaux, L.; Ishido, T. Electrokinetics in earth sciences: A tutorial. *Int. J. Geophys.* **2012**, *2012*, 286107. [[CrossRef](#)]
24. Guillaume, C.L.; Gregoryanz, E.; Degtyareva, O.; McMahon, M.I.; Hanfland, M.; Evans, S.; Guthrie, M.; Sinogeikin, S.V.; Mao, H. Cold melting and solid structures of dense lithium. *Nat. Phys.* **2011**, *7*, 211–214. [[CrossRef](#)]
25. Zheng, Y.; Ding, L.; Ye, H.; Chen, Z. Vibration-induced property change in the melting and solidifying process of metallic nanoparticles. *Nanoscale Res. Lett.* **2017**, *12*, 308. [[CrossRef](#)] [[PubMed](#)]
26. Hixson, E.; Kahlbau, J. Quincke-Tube Acoustic Filter for Fluid Ducts. *J. Acoust. Soc. Am.* **1963**, *35*, 1895. [[CrossRef](#)]
27. Lato, T.; Mohany, A. Passive damping of pressure pulsations in pipelines using Herschel-Quincke tubes. *J. Sound Vib.* **2019**, *448*, 160–177. [[CrossRef](#)]
28. Hassaan, G.A. Mechanical Engineering in Ancient Egypt, Part XIII: Stone Vessels (Predynastic to Old Kingdom Periods). *Int. J. Recent Eng. Sci. (IJRES)* **2016**, *19*, 14–24.
29. Liu, X.; Yu, C.; Xin, F. Gradually perforated porous materials backed with Helmholtz resonant cavity for broadband low-frequency sound absorption. *Compos. Struct.* **2021**, *263*, 113647. [[CrossRef](#)]
30. D’Alessandro, L.; Belloni, E.; Ardito, R.; Braghin, F.; Corigliano, A. Mechanical low-frequency filter via modes separation in 3D periodic structures. *Appl. Phys. Lett.* **2017**, *111*, 231902. [[CrossRef](#)]
31. Davidovits, J.; Morris, M. *Why the Pharaohs Built the Pyramids with Fake Stones*; Institut Géopolymère-Geopolymer Institute-Saint-Quentin (FranceEditor): Joseph Davidovits, France, 2009; ISBN 9782951482043.
32. Breitner, R.; Houdin, J.P.; Brier, B. A Computer Simulation to Determine When the Beams in the King’s Chamber of the Great Pyramid Cracked. *J. Am. Res. Cent. Egypt* **2012**, *48*, 23–33.
33. Bui, H.D. *Imaging the Cheops Pyramid*; Springer Science & Business Media: Cham, Switzerland, 2011; Volume 182.
34. Lheureux, P. Analyse Critique de la Rampe Interne Imaginée par Jean-Pierre Houdin. 2010. Available online: <https://pyramide.franceserv.com/analyse-critique-de-la-rampe-interne-imaginée-par-jean-pierre-houdin/> (accessed on 29 August 2022).
35. Bui, H.; Lakshmanan, J.; Montluçon, J.; Erling, J.; Nakhla, C. The Application of microgravity survey in the endoscopy of ancient monuments. In *The Engineering Geology of Ancient Works, Monuments and Historical Sites, Athens*; CRC Press: Boca Raton, FL, USA, 1988.
36. Ivashov, S.; Bechtel, T.; Razevig, V.; Capineri, L.; Inagaki, M. A proposed radar method for non-destructive investigation of Egyptian pyramids. *Insight-Non Test. Cond. Monit.* **2021**, *63*, 12–19. [[CrossRef](#)]
37. Yoshimura, S. Non-Destructive Pyramid Investigations (1), By Electromagnetic Wave Method. *Stud. Egypt. Cult.* **1987**, *6*, 61.

38. Bross, A.D.; Dukes, E.; Ehrlich, R.; Fernandez, E.; Dukes, S.; Gobashy, M.; Jamieson, I.; La Riviere, P.J.; Liu, M.; Marouard, G.; et al. Tomographic Muon Imaging of the Great Pyramid of Giza. *arXiv* **2022**, arXiv:2202.08184.
39. Aly, S.; Assran, Y.; Bonneville, A.; ElMahdy, B.; Kouzes, R.T.; Lintereur, A.; Mahrous, A.; Mostafanezhad, I.; Pang, R.; Rotter, B.; et al. Simulation Studies of a Novel Muography Detector for the Great Pyramids. *arXiv* **2022**, arXiv:2202.07434.
40. Alvarez, L.W.; Anderson, J.A.; El Bedwei, F.; Burkhard, J.; Fakhry, A.; Girgis, A.; Goneid, A.; Hassan, F.; Iverson, D.; Lynch, G.; et al. Search for hidden chambers in the pyramids. *Science* **1970**, *167*, 832–839. [[CrossRef](#)]
41. Morishima, K.; Kuno, M.; Nishio, A.; Kitagawa, N.; Manabe, Y.; Moto, M.; Takasaki, F.; Fujii, H.; Satoh, K.; Kodama, H.; et al. Discovery of a big void in Khufu’s Pyramid by observation of cosmic-ray muons. *Nature* **2017**, *552*, 386–390. [[CrossRef](#)] [[PubMed](#)]
42. Pašteka, R.; Zahorec, P.; Papčo, J.; Mrlić, J.; Götze, H.J.; Schmidt, S. The discovery of the “muons-chamber” in the Great pyramid; could high-precision microgravimetry also map the chamber? *J. Archaeol. Sci. Rep.* **2022**, *43*, 103464. [[CrossRef](#)]
43. Odah, H.; Abdallatif, T.; El-Hemaly, I.; El-All, E.A. Gradiometer survey to locate the ancient remains distributed to the northeast of the Zoser Pyramid, Saqqara, Giza, Egypt. *Archaeol. Prospect.* **2005**, *12*, 61–68. [[CrossRef](#)]
44. Richardson, R.; Whitehead, S.; Ng, T.; Hawass, Z.; Pickering, A.; Rhodes, S.; Grieve, R.; Hildred, A.; Nagendran, A.; Liu, J.; et al. The “Djedi” robot exploration of the southern shaft of the Queen’s chamber in the great Pyramid of Giza, Egypt. *J. Field Robot.* **2013**, *30*, 323–348. [[CrossRef](#)]
45. Evans, D.L.; Farr, T.G. The use of interferometric synthetic aperture radar (InSAR) in archaeological investigations and cultural heritage preservation. In *Remote Sensing in Archaeology*; Springer: New York, NY, USA, 2006; pp. 89–102.
46. Chen, F.; Lasaponara, R.; Masini, N. An overview of satellite synthetic aperture radar remote sensing in archaeology: From site detection to monitoring. *J. Cult. Herit.* **2017**, *23*, 5–11. [[CrossRef](#)]
47. Adams, R.E.; Brown, W.E.; Culbert, T.P. Radar mapping, archeology, and ancient Maya land use. *Science* **1981**, *213*, 1457–1468. [[CrossRef](#)] [[PubMed](#)]
48. Brichieri-Colombi, S. A spurred spiral ramp for the great pyramid of giza. *PalArch’s J. Archaeol. Egypt/Egyptol.* **2020**, *17*, 1–20.
49. Biondi, F. COSMO-SkyMed staring spotlight SAR data for micro-motion and inclination angle estimation of ships by pixel tracking and convex optimization. *Remote Sens.* **2019**, *11*, 766.
50. Biondi, F.; Addabbo, P.; Orlando, D.; Clemente, C. Micro-motion estimation of maritime targets using pixel tracking in COSMO-SkyMed synthetic aperture radar data—An operative assessment. *Remote Sens.* **2019**, *11*, 1637. [[CrossRef](#)]
51. Bovenga, F.; Giacovazzo, V.M.; Refice, A.; Veneziani, N. Multichromatic analysis of InSAR data. *IEEE Trans. Geosci. Remote Sens.* **2013**, *51*, 4790–4799. [[CrossRef](#)]
52. Biondi, F.; Addabbo, P.; Clemente, C.; Ullo, S.L.; Orlando, D. Monitoring of Critical Infrastructures by Micromotion Estimation: The Mosul Dam Destabilization. *IEEE J. Sel. Top. Appl. Earth Obs. Remote Sens.* **2020**, *13*, 6337–6351. [[CrossRef](#)]
53. Chen, H.P. *Structural Health Monitoring of Large Civil Engineering Structures*; John Wiley & Sons: Hoboken, NJ, USA, 2018.
54. Biondi, F.; Addabbo, P.; Ullo, S.L.; Clemente, C.; Orlando, D. Perspectives on the structural health monitoring of bridges by synthetic aperture radar. *Remote Sens.* **2020**, *12*, 3852. [[CrossRef](#)]
55. Biondi, F.; Clemente, C.; Orlando, D. An Atmospheric Phase Screen Estimation Strategy Based on Multichromatic Analysis for Differential Interferometric Synthetic Aperture Radar. *IEEE Trans. Geosci. Remote Sens.* **2019**, *57*, 7269–7280. [[CrossRef](#)]
56. Ferretti, A.; Prati, C.; Rocca, F. Permanent scatterers in SAR interferometry. *IEEE Trans. Geosci. Remote Sens.* **2001**, *39*, 8–20. [[CrossRef](#)]
57. Costantini, M.; Farina, A.; Zirilli, F. A fast phase unwrapping algorithm for SAR interferometry. *IEEE Trans. Geosci. Remote Sens.* **1999**, *37*, 452–460. [[CrossRef](#)]
58. Ullo, S.L.; Addabbo, P.; Di Martire, D.; Sica, S.; Fiscante, N.; Cicala, L.; Angelino, C.V. Application of DInSAR Technique to High Coherence Sentinel-1 Images for Dam Monitoring and Result Validation Through In Situ Measurements. *IEEE J. Sel. Top. Appl. Earth Obs. Remote Sens.* **2019**, *12*, 875–890. [[CrossRef](#)]
59. Chen, V.C.; Li, F.; Ho, S.S.; Wechsler, H. Micro-Doppler effect in radar: Phenomenon, model, and simulation study. *IEEE Trans. Aerosp. Electron. Syst.* **2006**, *42*, 2–21. [[CrossRef](#)]
60. Corbett, B.; Andre, D.; Finnis, M. Localising vibrating scatterer phenomena in synthetic aperture radar imagery. *Electron. Lett.* **2020**, *56*, 395–398. [[CrossRef](#)]
61. Reigber, A.; Moreira, A. First demonstration of airborne SAR tomography using multibaseline L-band data. *IEEE Trans. Geosci. Remote Sens.* **2000**, *38*, 2142–2152. [[CrossRef](#)]
62. Fornaro, G.; Pauciullo, A. LMMSE 3-D SAR Focusing. *IEEE Trans. Geosci. Remote Sens.* **2009**, *47*, 214–223. [[CrossRef](#)]
63. Zhu, X.X.; Bamler, R. Very High Resolution Spaceborne SAR Tomography in Urban Environment. *IEEE Trans. Geosci. Remote Sens.* **2010**, *48*, 4296–4308. [[CrossRef](#)]
64. Biondi, F. Scanning inside volcanoes with synthetic aperture radar echography tomographic Doppler imaging. *Remote Sens.* **2022**, *14*, 3828. [[CrossRef](#)]
65. Raney, R.K. Synthetic aperture imaging radar and moving targets. *IEEE Trans. Aerosp. Electron. Syst.* **1971**, *AES-7*, 499–505. [[CrossRef](#)]
66. Ouchi, K. On the multilook images of moving targets by synthetic aperture radars. *IEEE Trans. Antennas Propag.* **1985**, *33*, 823–827. [[CrossRef](#)]
67. Curlander, J.C.; McDonough, R.N. *Synthetic Aperture Radar: Systems and Signal Processing*; Wiley: New York, NY, USA, 1991.
68. Tufillaro, N.B. Nonlinear and chaotic string vibrations. *Am. J. Phys.* **1989**, *57*, 408–414. [[CrossRef](#)]

69. Li, B.; Liu, R.; Cong, Q.; Guo, H.; Lin, Q. Stress Superposition Method and free vibration of corner tensioned rectangular thin membranes. *Thin-Walled Struct.* **2021**, *159*, 107201. [[CrossRef](#)]
70. Marini, B. Real time muography simulator for scanpyramids mission. In Proceedings of the ACM SIGGRAPH 2018 Talks, Vancouver, BC, Canada, 12–16 August 2018; pp. 1–2.
71. Blidenberg, V.; Malherbe, A.; Rouhen, C.; Younsi, N. 3D Technology Solves the Mystery of the Great Pyramid. Available online: <https://www10.mcadcafe.com/nbc/articles/> (accessed on 29 August 2022).
72. MS Windows NT Kernel Description. Available online: <https://ilfattstorico.com/2016/10/18/camere-segrete-nella-piramide-di-cheope-i-primi-dubbi/> (accessed on 30 September 2010).
73. Whissell, P.; Persinger, M. Developmental effects of perinatal exposure to extremely weak 7 Hz magnetic fields and nitric oxide modulation in the Wistar albino rat. *Int. J. Dev. Neurosci.* **2007**, *25*, 433–439. [[CrossRef](#)] [[PubMed](#)]
74. St-Pierre, L.; Parker, G.; Bubenik, G.; Persinger, M. Enhanced mortality of rat pups following inductions of epileptic seizures after perinatal exposures to 5 nT, 7 Hz magnetic fields. *Life Sci.* **2007**, *81*, 1496–1500. [[CrossRef](#)] [[PubMed](#)]
75. Mulligan, B.P.; Persinger, M.A. Experimental simulation of the effects of sudden increases in geomagnetic activity upon quantitative measures of human brain activity: Validation of correlational studies. *Neurosci. Lett.* **2012**, *516*, 54–56. [[CrossRef](#)] [[PubMed](#)]
76. Jana, D. The great pyramid debate: Evidence from detailed petrographic examinations of casing stones from the Great Pyramid of Khufu, a natural limestone from Tura, and a man-made (geopolymeric) limestone. In Proceedings of the 29th Conference on Cement Microscopy, Quebec City, QC, Canada, 21–24 May 2007; Volume 207, p. 266.
77. MS Windows NT Kernel Description. 1999. Available online: <https://8916898.blogspot.com/2014/06/the-scirocco-infrasound-vibroacoustic.html> (accessed on 14 June 2014).